J|A|C|S
ARTICLES

Published on Web 11/22/2010

Compound ES of Dehaloperoxidase Decays via Two Alternative Pathways Depending on the Conformation of the Distal Histidine

Matthew K. Thompson,[†] Stefan Franzen,[†] Reza A. Ghiladi,[†] Brandon J. Reeder,[¶] and Dimitri A. Svistunenko*[,¶]

Department of Chemistry, North Carolina State University, Box 8204, Raleigh, North Carolina 27695-8204, United States, and Department of Biological Sciences, University of Essex, Colchester CO4 3SQ, United Kingdom

Received July 26, 2010; E-mail: svist@essex.ac.uk

Abstract: Dehaloperoxidase (DHP) is a respiratory hemoglobin (Hb) that has been shown to catalyze the conversion of trihalophenols to dihaloquinones in the presence of hydrogen peroxide. Ferric heme states of the resting DHP and the free radical intermediates formed under H_2O_2 treatment were studied by low-temperature electron paramagnetic resonance spectroscopy in the range of reaction times from 50 ms to 2 min at three different pH values. Two high-spin ferric heme forms were identified in the resting enzyme and assigned to the open and closed conformations of the distal histidine, His55. Two free radicals were found in DHP activated by H_2O_2: the radical associated with Compound ES (the enzyme with the heme in the oxoferryl state and a radical on the polypeptide chain) has been assigned to Tyr34, and the other radical has been assigned to Tyr38. The Tyr34 radical is formed with a very high relative yield (almost 100% of heme), atypical of other globins. High-performance liquid chromatography analysis of the reaction products showed a pH-dependent formation of covalent heme-to-protein cross-links. The stable DHP Compound RH, formed under H_2O_2 in the absence of the trihalophenol substrates, is proposed to be a state with the ferric heme covalently cross-linked to Tyr34. A kinetic model of the experimental data suggests that formation of Compound RH and formation of the Tyr38 radical are two alternative routes of Compound ES decay. Which route is taken depends on the conformation of His55: in the less populated closed conformation, the Tyr38 radical is formed, but in the major open conformation, Compound ES decays, yielding Compound RH, a product of safe termination of the two oxidizing equivalents of H_2O_2 when no substrate is available.

1. Introduction

Dehaloperoxidase hemoglobin (DHP), originally isolated from the terebellid polychaete *Amphitrite ornata*, is the first characterized hemoglobin known to have natural peroxidase function. When activated with hydrogen peroxide, DHP catalyzes the overall two-electron oxidation of 2,4,6-trihalophenol (2,4,6-TXP) to the corresponding 2,6-dihaloquinone (Scheme 1).[1] *A. ornata* cohabits benthic ecosystems with organisms such as *Thelespus crispis* and *Notomastus lobatus* that secrete brominated aromatics as predatory defense mechanisms.[2−4] To survive the toxic buildup, the coelomic oxygen-binding hemoglobin in *A. ornata* has evolved to perform a dehaloperoxidase function that results in a decrease in the concentration of toxic 2,4,6-TXP. DHP has a typical globin fold but a low amino acid sequence homology with other members of the globin family.[5] Two isoforms of DHP are found in *A. ornata* (DHP A and DHP B), both of which can bind oxygen reversibly.[6] The occurrence of globins in annelids is known to occur in two general contexts. First, a monomeric hemoglobin is observed in the coelom. Second, a giant hemoglobin is found in the tentacles and other compartments outside the coelom.[7] As a peroxidase, DHP acts 2 orders of magnitude faster than myoglobin (Mb)[8] and only an order of magnitude slower than horseradish peroxidase (HRP).[9] Thus, DHP lies in a unique median, sharing structural homology with globins and peroxidase activity with HRP.

Six available X-ray structures of DHP[5,10−12] demonstrate that the distal histidine, His55, may adopt an open (outside the distal pocket) or closed (inside the pocket) conformation. This high flexibility of the distal histidine has been implicated in the mechanism of switching between oxygen storing and peroxidase activity.[11] The first X-ray crystal structure of DHP showed the substrate analogue 4-iodophenol bound in the distal pocket with His55 pushed into the open conformation.[5] This led to the proposal that the distal pocket is the substrate-binding site.

Scheme 1

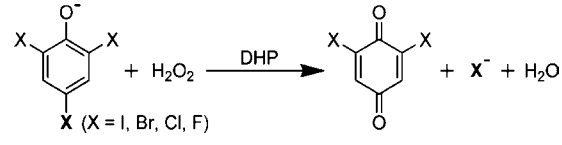

[†] North Carolina State University.
[¶] University of Essex.

(1) Chen, Y. P.; Woodin, S. A.; Lincoln, D. E.; Lovell, C. R. *J. Biol. Chem.* **1996**, *271*, 4609–4612.

However, structural, spectroscopic, and kinetic data[13−15] suggest the existence of an external binding site, while binding in the internal site, in fact, inhibits peroxidase function. Recently, Thompson et al. demonstrated that DHP exhibits nonclassical competitive inhibition, in which the inhibitor and substrate pair communicate between the internal and external binding sites, respectively, through two conformations of the distal histidine.[16]

Upon activation by H_2O_2, DHP is converted to the oxoferryl heme state, with a free radical on the globin assigned to a tyrosine.[17] This state of DHP was interpreted as Compound ES by analogy with cytochrome *c* peroxidase (C*c*P)[18] and was implicated in substrate oxidation. In the absence of trihalophenol substrates, Compound ES evolves stoichiometrically into a new optically detectable stable species termed Compound RH (*reversible heme* intermediate). This compound has not been reported for other heme proteins. It has an optical spectrum more characteristic of the ferric state of the heme, rather than the oxoferryl, but with a red shift of the Soret band.[17] Interestingly, Compound RH can be reduced by external reductants to completely functional ferrous DHP, which combines with oxygen to give Compound III (an oxyferrous state).[17]

The electron paramagnetic resonance (EPR) spectra of the radical associated with Compound ES were shown to be different when the activation was conducted at pH 5 and pH 7.[17] This raises the question of whether the structural properties of Compound ES change with pH or a parallel process is leading to formation of a different free radical on the enzyme. This paper is aimed at elucidation of the mechanism of free radical formation on DHP when the enzyme is treated with H_2O_2. Herein we show that two different tyrosyl radicals, Tyr34$^{\bullet}$ and Tyr38$^{\bullet}$, are responsible for the pH dependence of the free radical EPR spectrum, but only the Tyr34$^{\bullet}$ radical is associated with Compound ES. The other radical is formed during one of the two alternative routes of Compound ES decay.

2. Experimental Section

2.1. Materials. Buffer salts were purchased from Fisher Scientific. All other reagents were purchased from Sigma-Aldrich and used without further purification. DHP A[6] was studied in this paper.

2.2. 6XHis-Tagged DHP A Growth and Purification. Recombinant his-tagged wild-type DHP protein was expressed in *Escherichia coli* and purified as previously described.[14] All experiments in this report were conducted in 100 mM potassium phosphate buffer.

2.3. Hydrogen Peroxide Solutions. The H_2O_2 solution was prepared from a 30% reagent grade H_2O_2 solution from Fisher Chemicals to a final concentration of 15 mM for the stock solution. Aliquots of 15 mM H_2O_2 stock solution in 100 mM potassium phosphate buffer at pH 7 were stored in cryotubes at liquid nitrogen temperature. The cryotubes were thawed and diluted in 100 mM potassium phosphate buffer shortly before use. One cryotube was used for making no more than three or four freeze-quenched samples, which normally took no longer than 1 h. This protocol was followed in order to maintain the peroxide concentration constant during several hours of sample preparation sessions.

2.4. EPR Sample Preparation. Wilmad SQ EPR tubes (Wilmad Glass, Buena, NJ) were used for EPR samples. To minimize the effect that slightly different tube sizes might have on the quantitative results, only tubes with outer diameter 4.05 ± 0.07 mm and inner diameter 3.12 ± 0.04 mm (mean $\pm$ range) were selected for use. When a set of samples was prepared by freezing the same protein solution in the selected Wilmad SQ tubes, the random error in the EPR signal intensities was determined to be very low (1−3%).

The rapid freeze-quenching (RFQ) of the EPR samples was performed by a combined use of an Update Instrument (Madison, WI) mixing machine and a home-built apparatus for freezing the ejected mixtures on the surface of a rapidly rotating aluminum disk kept at liquid nitrogen temperature (see Supporting Information, SI.Methods.1). The freezing time achievable by this apparatus was calibrated by the method described elsewhere[19] based on azide binding to horse metmyoglobin (metMb), where the rate constant of the binding was determined optically by an Applied Photophysics SX18MV diode array spectrophotometer. DHP and H_2O_2 solutions were kept at 4 °C in the Update Instrument freeze-quenching apparatus and were mixed in the mixing chamber kept just outside the ice bath (at ca. 15 °C). The samples corresponding to the time points in the range of 50−300 ms were made using aging hoses of variable length. For longer reaction times, a delay was used between two pushes of the ram of the freeze-quenching apparatus. The sample frozen on the cold disk was transferred to a funnel attached to an EPR tube and packed with a Teflon-tipped stainless steel rod. The packing factor was found to be persistently close to 50% ($\pm$4%). The freeze-quenched samples, when packed, were of variable length, sometimes shorter than the active zone of the resonators. This affected the intensity of the EPR signals. To make a correction for this effect, we used the sample length-specific coefficients obtained as described in the Supporting Information (SI.Methods.2).

2.5. EPR Spectra Measurement and Processing. All EPR spectra were measured on a Bruker EMX EPR spectrometer (X-band) at a modulation frequency of 100 kHz. Accurate *g*-values were obtained using the built-in microwave frequency counter and a 2,2-diphenyl-1-picrylhydrazyl powder standard, the *g*-value for which is $g = 2.0037 \pm 0.0002$.[20] A spherical high-quality Bruker resonator SP9703 and an Oxford Instruments liquid helium system

(2) Woodin, S. A.; Marinelli, R. L.; Lincoln, D. E. *J. Chem. Ecol.* **1993**, *19*, 517–530.
(3) Fielman, K. T.; Woodin, S. A.; Walla, M. D.; Lincoln, D. E. *Mar. Ecol.: Prog. Ser.* **1999**, *181*, 1–12.
(4) Lincoln, D. E.; Fielman, K. T.; Marinelli, R. L.; Woodin, S. A. *Biochem. Systemat. Ecol.* **2005**, *33*, 559–570.
(5) LaCount, M. W.; Zhang, E.; Chen, Y. P.; Han, K.; Whitton, M. M.; Lincoln, D. E.; Woodin, S. A.; Lebioda, L. *J. Biol. Chem.* **2000**, *275*, 18712–18716.
(6) Han, K.; Woodin, S. A.; Lincoln, D. E.; Fielman, K. T.; Ely, B. *Mar. Biotechnol. (NY)* **2001**, *3*, 287–292.
(7) Mangum, C. P.; Woodin, B. R.; Bonaventura, C.; Sullivan, B.; Bonaventura, J. *Comp. Biochem. Physiol.* **1975**, *51A*, 281–294.
(8) Osborne, R. L.; Coggins, M. K.; Walla, M.; Dawson, J. H. *Biochemistry* **2007**, *46*, 9823–9829.
(9) Belyea, J.; Gilvey, L. B.; Davis, M. F.; Godek, M.; Sit, T. L.; Lommel, S. A.; Franzen, S. *Biochemistry* **2005**, *44*, 15637–15644.
(10) de Serrano, V.; Chen, Z.; Davis, M. F.; Franzen, S. *Acta Crystallogr. D: Biol. Crystallogr.* **2007**, *63*, 1094–1101.
(11) Chen, Z.; de Serrano, V.; Betts, L.; Franzen, S. *Acta Crystallogr. D: Biol. Crystallogr.* **2009**, *65*, 34–40.
(12) de Serrano, V.; D'Antonio, J.; Franzen, S.; Ghiladi, R. A. *Acta Crystallogr. D: Biol. Crystallogr.* **2010**, *66*, 529–238.
(13) Nienhaus, K.; Nickel, E.; Davis, M. F.; Franzen, S.; Nienhaus, G. U. *Biochemistry* **2008**, *47*, 12985–12994.
(14) Davis, M. F.; Gracz, H.; Vendeix, F. A.; de Serrano, V.; Somasundaram, A.; Decatur, S. M.; Franzen, S. *Biochemistry* **2009**, *48*, 2164–2172.
(15) Davis, M. F.; Bobay, B. G.; Franzen, S. *Biochemistry* **2010**, *49*, 1199–206.
(16) Thompson, M. K.; Davis, M. F.; de Serrano, V.; Nicoletti, F. P.; Howes, B. D.; Smulevich, G.; Franzen, S. *Biophys. J.* **2010**, *99*, 1586–1595.
(17) Feducia, J.; Dumarieh, R.; Gilvey, L. B.; Smirnova, T.; Franzen, S.; Ghiladi, R. A. *Biochemistry* **2009**, *48*, 995–1005.
(18) Sivaraja, M.; Goodin, D. B.; Smith, M.; Hoffman, B. M. *Science* **1989**, *245*, 738–740.
(19) Cherepanov, A. V.; De Vries, S. *Biochim. Biophys. Acta* **2004**, *1656*, 1–31.
(20) Weil, J. A.; Bolton, J. R.; Wertz, J. E. *Electron paramagnetic resonance: Elementary theory and practical applications*; John Wiley & Sons, Inc.: New York, 1994.

were used to measure the low-temperature EPR spectra. The EPR spectra of the blank samples (frozen water) were subtracted from the EPR spectra of the enzyme samples to eliminate the baseline caused by the resonator's walls, quartz insert, or quartz EPR tube.

The freeze-quenched control samples were obtained by mixing a DHP solution with buffer. The $g_{||} = 2$ component of the high-spin (HS) ferric heme signal, obtained from the DHP control samples, has been subtracted from the EPR spectra of the protein radicals formed under peroxide treatment using individual coefficients of subtraction for each spectrum as described elsewhere.[21] Thus, the free radical spectra presented in this paper are not contaminated with the HS ferric heme DHP EPR signal.

To measure intensities of overlapping EPR signals in a composite EPR spectrum, the procedure of spectral subtraction with a variable coefficient was used.[22,23] Different EPR samples are measured at slightly different microwave frequencies because of the variation in the physical characteristics of the EPR tubes. Therefore, the same EPR signal in two different EPR samples can appear at slightly different values of the magnetic field. To increase the accuracy of the spectral subtraction, this error has been corrected by shifting each experimental spectrum to the left or to the right along the magnetic field in accordance with the difference between the frequency used to record an individual spectrum and a frequency value chosen as a standard for the whole array of experimental spectra. Thus, a good alignment of all EPR spectra on the magnetic field axis has been achieved. Figure S5 (Supporting Information, SI.Methods.3) illustrates the effect of the spectral shifting procedure on a set of spectra obtained from different samples. It should be noted that the spectral position correction based on the microwave frequency value will not have an accurate outcome (e.g., as shown in Figure S5) if the magnetic field is drifting. It normally takes several hours for the EMX spectrometer to achieve stable magnetic field characteristics. Therefore, all our EPR experiments were performed after the spectrometer had a considerable warm-up time (2−3 days).

2.6. EPR Spectra Simulation. Tyrosyl radical EPR spectra were simulated using SimPow6.[24] The Tyrosyl Radical Spectra Simulation Algorithm (TRSSA)[25] was used to generate the EPR spectral simulation parameters on an input of only two parameters, the phenoxyl ring rotation angle and the spin density on atom C1 of the radical.

2.7. Assignment of Tyrosyl Radicals to Specific Tyrosine Residues. The Phenol Ring Rotation Angle Database[26] has been used to identify the tyrosine residues in DHP with the same, or similar, rotational conformation of the phenol group (the ring rotation angle) as the conformation determined from the simulation of the tyrosyl radical EPR spectrum.

2.8. Kinetic Modeling. Time dependences of the concentration of total ferric heme state and total free radical, at three different pH values, were modeled using Microsoft Office Excel 2007, while the Excel Solver tool was used to optimize the rate constants by finding the minimum of the average distance between experimental and calculated values. Three average distance parameters attributable to different pH value series were added together to a single value which has been minimized during global optimization.

2.9. Reverse-Phase HPLC. The reverse-phase HPLC method for the identification of heme-protein cross-links was adapted from that of Osawa and Korzekwa.[27] DHP (80 μM) was reacted with H_2O_2 (0−1600 μM) in 15 mM sodium acetate buffer (pH 5.0) or sodium phosphate buffer (pH 6.0 or 7.0). The reaction was allowed to stand for at least 2 h prior to HPLC analysis. Samples were analyzed on an Agilent HP1100 HPLC equipped with a diode array spectrophotometer and fitted with a Zorbax StableBond 300 C3 column (250 mm × 4.6 mm) with a 12 mm × 4.6 mm guard column. Solvents were (A) water containing 0.1% trifluoroacetic acid (TFA) and (B) acetonitrile containing 0.1% TFA. The gradient was initially 35% solvent B, stable for 10 min, increasing to 37% solvent B over 5 min. This was increased to 40% solvent B over 1 min and then to 43% solvent B over 10 min. The flow rate was 1 mL min^{-1}, and the temperature was 25 °C. The concentration of heme-to-protein cross-linking was determined by integrating the heme-to-protein cross-linked HPLC peak at 400 nm and comparing the area to a standard.

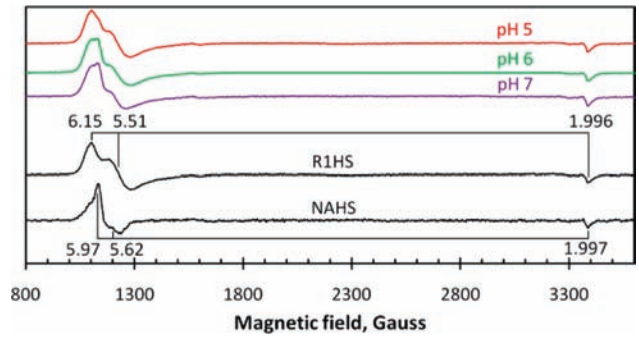

Figure 1. EPR spectra of ferric DHP at different pH values and the result of their deconvolution into two individual HS ferric heme EPR signals, rhombic type 1 (R1HS) and nearly axial (NAHS). The spectra were obtained at 10 K from the samples made by freeze-quenching 80 μM DHP at the indicated pH values mixed with equal volumes of buffer to give a final concentration of 40 μM. All spectra are plotted at similar amplitudes for comparative viewing. The instrumental conditions were as follows: microwave frequency $\nu_{MW} = 9.471$ GHz, microwave power $P = 3.18$ mW, modulation frequency $\nu_m = 100$ kHz, modulation amplitude $A_m = 5$ G, time constant $\tau = 82$ ms, scan rate $\upsilon = 22.6$ G s^{-1}, number of scans per spectrum NS = 1. The principal g-factors of the signals R1HS and NAHS are indicated.

3. Results

3.1. Heme States in the Resting (Ferric) Enzyme. The EPR spectra of rapidly freeze-quenched DHP in the resting (ferric) state at three different pH values are shown in Figure 1. While no low-spin ferric heme forms are seen in the spectra, the EPR signal of the HS form in the $g = 6$ region shows a slightly different line shape at pH 5, 6, and 7. The differences were used to deconvolute the signal into two components: a rhombic component, with the g-values g_1 and g_2 well separated (R1HS, rhombic type 1 high spin), and a nearly axial component, i.e., when the difference between g_1 and g_2 is small (NAHS, nearly axial high spin). The R1HS EPR signal ($g_1 = 6.15$, $g_2 = 5.51$, $g_3 = 1.996$) was obtained as a difference spectrum, R1HS = (pH 5) − 0.38(pH 7). The NAHS signal ($g_1 = 5.97$, $g_2 = 5.62$, $g_3 = 1.997$) was constructed as NAHS = (pH 7) − 0.69(pH 5). The coefficients of the subtractions were determined empirically to yield the best pure line shapes of the individual EPR signals.

The relative concentrations of the heme states responsible for the two signals, R1HS and NAHS, were estimated by measuring the relative intensities of the signals in the DHP spectra at pH 5, 6, and 7 and expressing them in common units

(21) Svistunenko, D. A.; Reeder, B. J.; Wankasi, M. M.; Silaghi-Dumitrescu, R.-L.; Cooper, C. E.; Rinaldo, S.; Cutruzzolà, F.; Wilson, M. T. *Dalton Trans.* **2007**, 840–850.
(22) Svistunenko, D. A. *Biochim. Biophys. Acta* **2005**, *1707*, 127–155.
(23) Svistunenko, D. A.; Davies, N.; Brealey, D.; Singer, M.; Cooper, C. E. *Biochim. Biophys. Acta* **2006**, *1757*, 262–272.
(24) Nilges, M. J.; Matteson, K.; Bedford, R. L. In *ESR Spectroscopy in Membrane Biophysics*; Hemminga, M. A., Berliner, L., Eds.; Biological Magnetic Resonance *27*; Springer: New York, 2007; Appendix 2.
(25) Svistunenko, D. A.; Cooper, C. E. *Biophys. J.* **2004**, *87*, 582–595.
(26) Svistunenko, D., 2004, http://privatewww.essex.ac.uk/~svist/lev1/tyrdb/home.shtml.
(27) Osawa, Y.; Korzekwa, K. *Proc. Natl. Acad. Sci. U.S.A.* **1991**, *88*, 7081–7085.

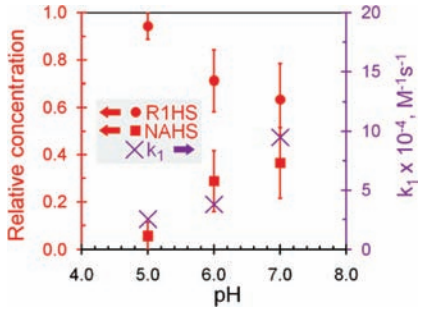

Figure 2. Relative concentration (left axis) of the two HS ferric heme forms in DHP, rhombic type 1 (R1HS) and nearly axial (NAHS), at three different pH values. The error bars indicate maximal deviation from the average determined on the basis of three independent measurements. The concentration units are normalized to give the total concentration equal to unity. Also shown are the values of the rate constants k_1 (Compound ES formation, right axis) that have been obtained from the kinetic model described in section 3.2.5.

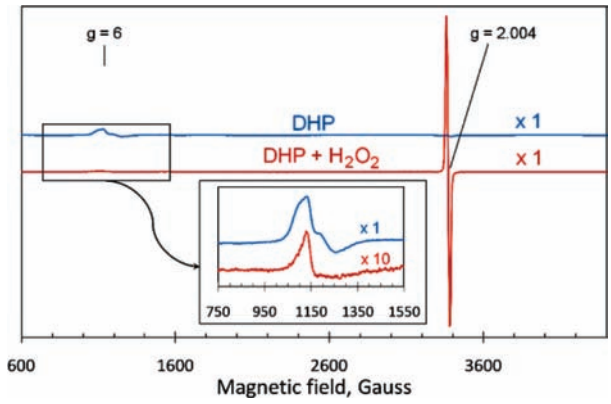

Figure 3. EPR spectra of 40 μM DHP reacted with 150 μM H_2O_2 and freeze-quenched 0.5 s after mixing (all concentrations are final, pH 7). The control sample was obtained by mixing equal volumes of 80 μM DHP and pH 7 buffer and freeze-quenching 50 ms after mixing. Inset shows the g = 6 area in greater detail, with the H_2O_2-treated spectrum magnified by a factor of 10. The spectra were recorded at 10 K at the same instrumental conditions as specified in the Figure 1 legend.

when the values of second integrals of R1HS and NAHS were taken into account. The result is presented in Figure 2, which shows a stoichiometric transition of R1HS into NAHS as pH increases.

3.2. DHP Reacting with H_2O_2. When hydrogen peroxide is added to DHP, the paramagnetic ferric heme state is transformed to the EPR-silent oxoferryl form, leading to a decrease of the g = 6 signal intensity in the EPR spectrum. At the same time, a protein-bound free radical is formed, resulting in the appearance of a g = 2.004 EPR signal (Figure 3). This state of DHP with a protein-bound free radical was first observed by Feducia et al. and interpreted as Compound ES.[17]

3.2.1. Concentration of the Ferric Heme and the Free Radicals as a Function of Reaction Time. Kinetic dependences of the ferric heme state and the free radical concentrations were studied in DHP reacting with H_2O_2 at three different pH values (Figures 4 and 5).

The concentrations of the ferric heme state were measured from the intensities of the HS ferric heme EPR signal and, in the absence of detectable low-spin forms, were assumed to reflect the total ferric heme concentration. The average intensity of the HS ferric heme EPR signals in the control samples (freeze-quenched on mixing with buffer containing no peroxide)

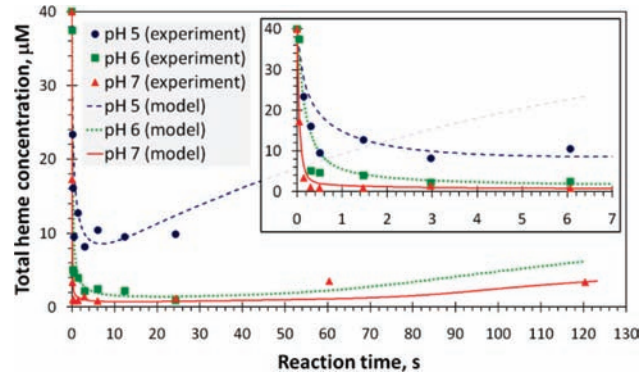

Figure 4. Kinetic dependences of total ferric heme state concentration in the course of the reaction of 40 μM ferric DHP with 120 μM H_2O_2, at pH 5, 6, and 7 (both concentrations are final). The ferric heme concentrations (symbols) were determined by EPR spectroscopy in the samples prepared by the RFQ method as described in the text. The lines are calculated from the kinetic model described in section 3.2.5.

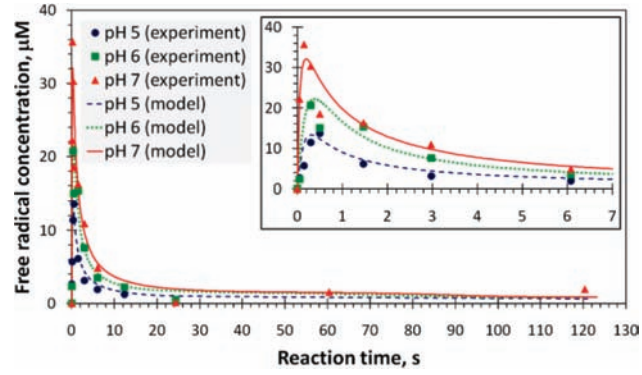

Figure 5. Kinetic dependences of total free radical concentration in the three pH series referred to in Figure 4. The EPR spectra of the free radicals detected in these series are given in Figure S6 (Supporting Information). Symbols represent the experimental results; the lines are generated by the same kinetic model used to plot the curves in Figure 4 (see section 3.2.5 for details).

was thus normalized to the initial ferric enzyme concentration determined optically (40 μM after 2-fold dilution). The small changes in the proportion of R1HS and NAHS (see section 3.2.2) were ignored in the measurements.

The total free radical concentrations were determined in common units of the second integral of the EPR spectra (Supporting Information, Figure S6, SI.Results.1), measured at low microwave power, after the g = 2 component of the HS ferric heme state (measured in the control, i.e., when no H_2O_2 was added) was subtracted as described elsewhere.[21] The subtraction coefficients for each spectrum were found from the kinetics of the HS forms shown in Figure 4. The integral values were then corrected for variable sample size, as described in section 2.4, and normalized to absolute concentration values using a Cu^{2+} concentration standard.

While reporting the "total free radical concentration" in Figure 5, we should note that the radical composition was not uniform in the series studied. The line shape of the free radical EPR signals was different in the different pH series. The line shape also changed during the reaction time. Generally, the resolution of the hyperfine structure in the free radical EPR spectrum becomes poorer as time progresses (Figure S6). In different pH series, the initial line shape persisted for different lengths of reaction time, i.e., for 0.5 s at pH 5, for 3 s at pH 6, and for 6 s at pH 7.

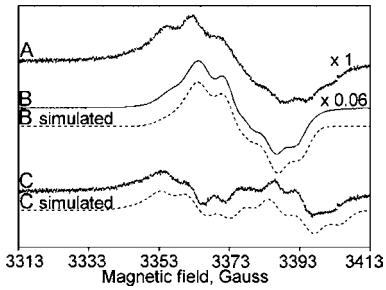

Figure 6. Line shapes of the free radical EPR spectra of the freeze-quenched samples of 40 μM DHP treated with 120 μM H_2O_2: (A) pH 5, 50 ms after mixing and (B) pH 7, 300 ms after mixing, multiplied by a factor of 0.06. The factor 0.06 was chosen empirically to construct a pure line shape of the signal C = A − B. Both the principal radical (B) and pH 5 radical (C) EPR signals were simulated as neutral tyrosyl radical spectra (dotted lines). The parameters of the simulation (Supporting Information, Tables S1 and S2) were found by TRSSA.[25]

The experimental kinetic dependences of the ferric heme and free radical at pH 5, 6, and 7 have been fitted by the dependences computed from a kinetic model (Figures 4 and 5). The model is described in section 3.2.5.

3.2.2. High-Spin Ferric Heme after H_2O_2 Addition. Although a significant decrease in the concentration of the HS ferric heme forms is seen during the reaction of DHP with H_2O_2, the relative proportion of the rhombic (R1HS) and nearly axial (NAHS) ferric heme forms after the addition of H_2O_2 is similar to the relative proportion before the addition of H_2O_2. This indicates that the two forms might be in a fast equilibrium. Two small but noticeable effects should be noted though. First, the relative concentration of the axial form is slightly higher in the samples of DHP reacting with H_2O_2 than in the resting (control) samples. Second, when the ferric heme starts to recover from the EPR-invisible oxoferryl form (e.g., 1 min after mixing, pH 7, Figure 4), a weak signal of a new rhombic HS ferric heme (type 2, R2HS) can be seen in the spectrum. It shows a slightly greater degree of rhombicity than R1HS and is characterized by the *g*-factors $g_1 = 6.39$ and $g_2 = 5.42$ (Supporting Information, Figure S7).

3.2.3. Identification of Two Different Hydrogen-Bonded Tyrosyl Radicals. Figure S6 demonstrates that the line shapes of the free radical EPR spectra of DHP treated with H_2O_2 are different at different pH values. The difference is particularly evident when the pH 5 and pH 7 series are compared. We used the procedure of spectral subtraction with a variable coefficient[22,23] to identify two different free radical EPR signals (Figure 6). One is present at all pH values studied and is particularly strong in the pH 7 spectra. We will refer to this EPR signal as that originating from *the principal free radical*. The other signal is generally of a much weaker intensity and is observable at pH 5 (henceforth referred to as the *pH 5 radical* signal).

The two EPR signals have been simulated as tyrosyl radical EPR spectra (Figure 6). The simulation parameters are given in the Supporting Information, Tables S1 and S2. Each of these two sets of 30 parameters has been found by TRSSA[22,25,28] when only two input parameters of the algorithm were varied. The optimal values of these two parameters for the two radicals are specified in Table 1.

Table 1. TRSSA[a] Input Parameters for the Simulation of the Tyrosyl Radical EPR Signals in Figure 6

	McConnell spin density on atom C1, ρ_{C1}	phenoxyl ring rotation angle θ, degrees[b]
principal radical (B)	0.400	45 (or 75)
pH 5 radical (C)	0.420	−8 (or −52)

[a] Tyrosyl Radical Spectra Simulation Algorithm. [b] There are always two values of rotation angle θ that give identical sets of simulation parameters.[25,29] See Supporting Information (SI.Results.2) for details.

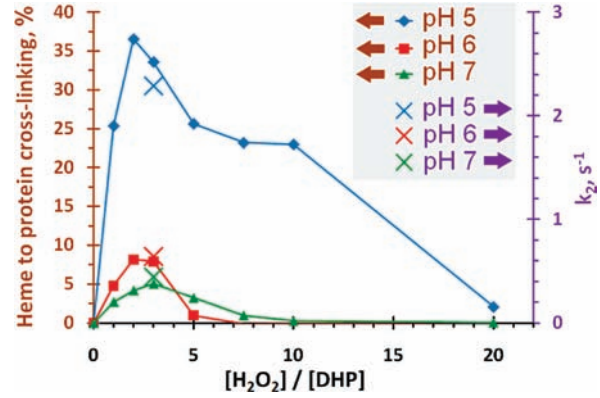

Figure 7. Effect of H_2O_2 molar excess over heme on the extent of heme-to-protein cross-link formation in 80 μM DHP (curves, left axis). The concentration of the heme-to-protein cross-links was determined by HPLC, and dependences at three different pH values are presented. Three crosses are related to the right axis and represent the rate constant k_2 of Compound ES to Compound RH conversion at the three pH values, as found from the kinetic model described in section 3.2.5.

The values of the spin density on C1 for the two radicals are both in the upper part of the range of values (0.35−0.42) for other protein-bound tyrosyl radicals.[25] This means that both tyrosyl radicals are hydrogen bonded. In fact, the value of 0.42 for the pH 5 radical is at the top of the range and indicates that the H-bond engaging this radical must be strong.

The principal tyrosyl radical, found in all three pH series, is characterized by the phenoxyl ring rotation angle of 45° or 75°. This angle in the pH 5 tyrosyl radical is either −8° or −52°. By using the Phenol Ring Rotation Angle Database,[26] an assignment of the radicals has been performed. The most likely site of the principal radical is either Tyr28 or Tyr34, and the most likely site of the pH 5 radical is Tyr38. For details of the analysis leading to this conclusion, see the Supporting Information, SI.Results.2.

3.2.4. Formation of Heme-to-Protein Cross-Links. Reverse-phase HPLC was employed to study the oxidation of the heme prosthetic group in the reaction of DHP with H_2O_2 (Supporting Information, Figure S8). The chromatograms obtained and the optical properties of the eluted fractions (Supporting Information, Figure S9) allowed identification of a DHP form in which the heme is covalently cross-linked to the globin. The H_2O_2 concentration profile of the cross-link formation is pH dependent, as shown in Figure 7.

3.2.5. Kinetic Model. The time dependences of the concentrations of total ferric heme and total free radical have been modeled (Figures 4 and 5) by calculating a kinetic evolution of ferric DHP reacting with H_2O_2. A set of 10 chemical reactions involving six reaction components was postulated:

$$\text{Fe(III)} + H_2O_2 \xrightarrow{k_1} \bullet\text{Fe(IV)} \quad (1)$$

(28) Svistunenko, D. A.; Jones, G. A. *Phys. Chem. Chem. Phys.* **2009**, *11*, 6600–6613.
(29) Svistunenko, D. A.; Wilson, M. T.; Cooper, C. E. *Biochim. Biophys. Acta* **2004**, *1655*, 372–380.

$$\bullet\text{Fe(IV)} \xrightarrow{k_2} \text{Fe(III)} \quad (2)$$

$$\bullet\text{Fe(IV)} \xrightarrow{k_3} \bullet\text{Fe(III)}\bullet \quad (3)$$

$$\text{Fe(IV)} \xrightarrow{k_4} \bullet\text{Fe(III)} \quad (4)$$

$$\bullet\text{Fe(IV)} + \bullet\text{Fe(IV)} \xrightarrow{k_5} \text{Fe(IV)} + \text{Fe(IV)} \quad (5)$$

$$\bullet\text{Fe(IV)} + \bullet\text{Fe(III)} \xrightarrow{k_6} \text{Fe(IV)} + \text{Fe(III)} \quad (6)$$

$$\bullet\text{Fe(IV)} + \bullet\text{Fe(III)}\bullet \xrightarrow{k_7} \text{Fe(IV)} + \bullet\text{Fe(III)} \quad (7)$$

$$\bullet\text{Fe(III)} + \bullet\text{Fe(III)} \xrightarrow{k_8} \text{Fe(III)} + \text{Fe(III)} \quad (8)$$

$$\bullet\text{Fe(III)} + \bullet\text{Fe(III)}\bullet \xrightarrow{k_9} \text{Fe(III)} + \bullet\text{Fe(III)} \quad (9)$$

$$\bullet\text{Fe(III)}\bullet + \bullet\text{Fe(III)}\bullet \xrightarrow{k_{10}} \bullet\text{Fe(III)} + \bullet\text{Fe(III)} \quad (10)$$

The rationales behind postulating these reactions, together with a number of assumptions made, are given in the Supporting Information, SI.Results.3. Briefly, reaction 1 describes formation of Compound ES. The latter decays via two alternative reactions, 2 and 3. Reaction 4 is a decay of the ferryl heme state into the "ferric + radical" state. Reactions 5−10 are six radical recombination reactions that can take place between three types of radical species in the model: a radical on DHP in the ferric heme state •Fe(III), a radical when DHP is in the ferryl state •Fe(IV), and a biradical DHP when the heme is ferric •Fe(III)•. For a time point of the evolution, the derivatives by time of the concentrations (rates) for each component were formulated via the rate constants and the components' concentrations. The concentration dependences on time (t) were then obtained by stepwise integration of the derivatives over the time range of choice (see details in Supporting Information, SI.Results.3 and the Excel file). The graphs showing the time dependences of the total free radical concentration and the total ferric heme state were combined as follows:

$$[\text{Total free radical}](t) = \bullet\text{Fe(III)}(t) + 2\bullet\text{Fe(III)}\bullet(t) + \bullet\text{Fe(IV)}(t)$$

$$[\text{Total ferric heme}](t) = \text{Fe(III)}(t) + \bullet\text{Fe(III)}(t) + \bullet\text{Fe(III)}\bullet(t)$$

The Excel file available in the Supporting Information allows visual monitoring of all constructed kinetic dependences on one screen. A change in any one of the 32 parameters (ten rate constants × three pH values + $[DHP]_0$ + $[H_2O_2]_0$) instantly produces change(s) in the calculated kinetic dependences. The initial DHP and H_2O_2 concentrations were not varied during the fitting process. The fitting procedure was based on minimizing the "target" parameters, the average absolute difference between experimental and calculated concentration values, defined for each pH series (T_{pH5}, T_{pH6}, and T_{pH7}) and for all three sets of data when optimizing the rate constants globally ($T = T_{pH5} + T_{pH6} + T_{pH7}$) (see details in Supporting Information, SI.Results.3). The constraints imposed on the rate constants have allowed diminishing of the 30D variable space down to 13 variables (see SI.Results.3). Table 2 presents the optimized values of the 30 rate constants that were used to plot the continuous lines in Figures 4 and 5. This set of rate constants produces the T parameter equal to 12.73 μM, which is, on average, 2.1 μM for each of the six experimental kinetic dependences modeled. We consider this a good accuracy of fitting for the case of total protein concentration of 40 μM. It is rather difficult to estimate classical errors of the rate constants in Table 2 because of uncertainty in the confidence level one might want to assume for a range of values for each k_i (i = 1, 2, ..., 10). It is possible, however, to determine the ranges of k_i values around their optimal points for which the target parameter T would be greater than $T_{optimal}$ by not more than a conventional value. Table 2 thus reports the ranges of k values that correspond to a maximal increase of T by 1 μM from the optimal value of 12.73 μM (see details in Supporting Information). These ranges of k values are given for the rate constants that have been varied during the optimization (k_1, k_2, k_4, and k_5), all other rate constants being their algebraic functions.

Table 2. Optimized Rate Constants of the Reactions Included in the Kinetic Model[a]

	pH 5	pH 6	pH 7
k_1, M^{-1} s^{-1}	$(2.53 \pm 0.18) \times 10^4$	$(3.78 \pm 2.46) \times 10^4$	$(9.47 \pm 0.94) \times 10^4$
k_2, s^{-1}	2.29 ± 0.09	0.64 ± 0.05	0.44 ± 0.79
k_3, s^{-1}	0.093	0.017	0.005
k_4, s^{-1}	0.009 ± 0.003	0.002 ± 0.002	0.001 ± 0.001
k_5, M^{-1} s^{-1}	$(14.52 \pm 1.94) \times 10^4$	$(5.11 \pm 1.17) \times 10^4$	$(2.81 \pm 2.68) \times 10^4$
k_6, M^{-1} s^{-1}	19.36×10^4	6.81×10^4	3.75×10^4
k_7, M^{-1} s^{-1}	38.72×10^4	13.63×10^4	7.50×10^4
k_8, M^{-1} s^{-1}	25.81×10^4	9.08×10^4	5.00×10^4
k_9, M^{-1} s^{-1}	51.63×10^4	18.17×10^4	10.01×10^4
k_{10}, M^{-1} s^{-1}	103.3×10^4	36.33×10^4	20.01×10^4

[a] The ranges of values are given for the rate constants varied during optimization, k_1, k_2, k_4 and k_5. Constants k_6-k_{10} are calculated as direct proportions of k_5; constants k_3 are calculated as k_2/Ak_1 where A is a constant.

4. Discussion

The enzyme activation can be represented as a sequence of transformations (Scheme 2) when the intermediates are the species detectable by optical and/or EPR spectroscopy. We now consider in detail the individual intermediates presented in Scheme 2 from the perspective of their spectroscopic properties.

4.1. Resting DHP: Relation between the Two HS Forms and the His55 in Open and Closed Conformations. We have found two HS ferric heme forms in the resting enzyme: a "nearly axial" signal and a rhombic one (NAHS and R1HS, Figure 1). These two forms are in a pH-dependent equilibrium, with R1HS being the acidic component and NAHS the alkaline component (Figure 2). The axial HS ferric heme state in the globins, such as Mb and Hb, has a water molecule coordinated by the distal histidine.[30−32] Therefore, we suggest that NAHS is a six-coordinate HS ferric heme state (6cHS) of DHP when the distal His55 is in the closed conformation coordinating a water molecule. Recently, Nicoletti et al. showed that binding of

(30) Peisach, J.; Blumberg, W. E.; Wittenberg, B. A.; Wittenberg, J. B. *J. Biol. Chem.* **1968**, *243*, 1871–1880.
(31) Peisach, J.; Blumberg, W. E.; Wittenberg, B. A.; Wittenberg, J. B.; Kampa, L. *Proc. Natl. Acad. Sci. U.S.A.* **1969**, *63*, 934–939.
(32) Svistunenko, D. A.; Sharpe, M. A.; Nicholls, P.; Blenkinsop, C.; Davies, N. A.; Dunne, J.; Wilson, M. T.; Cooper, C. E. *Biochem. J.* **2000**, *351*, 595–605.

Scheme 2

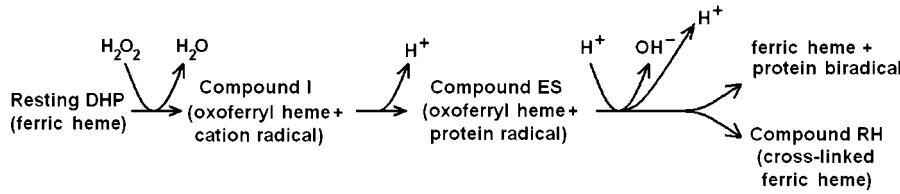

4-iodophenol to DHP produces a rhombic-type EPR line shape with g-values $g_1 = 6.22$, $g_2 = 5.50$, and $g_3 = 1.99$,[33] similar to the resting state R1HS shown in Figure 1 and Figure S7. Binding of 4-iodophenol in the distal heme side results in the distal His55 being pushed out of the pocket to the open conformation.[5] Therefore, we can assign R1HS to a five-coordinate HS ferric heme state (5cHS) of DHP in the open His55 conformation.

The forms R1HS (5cHS, open) and NAHS (6cHS, closed) are in a fast pH-dependent equilibrium in the resting state. The correlation of the His55 position and heme coordination has been observed by X-ray crystallography and nuclear magnetic resonance and resonance Raman spectroscopies.[10,11,14,15,33] The equilibrium is shifted toward R1HS as the pH is lowered (Figure 2) because of increasing protonation of the distal His55, which leads to the disruption of the hydrogen bonding to the water molecule in the sixth position of the heme iron. This displaces the distal His55 toward the open conformation, thus producing a 5cHS heme state. Another way to rationalize the effect of pH on the open/closed equilibrium is to think that one excessive positive charge on the histidine (at lower pH) makes it harder for the residue to approach the positively charged heme iron.

The equilibrium between the R1HS and NAHS ferric heme states seems to be slightly affected after the reaction starts: the decrease of R1HS upon H_2O_2 addition is marginally greater than the decrease of NAHS. In fact, the EPR spectra of the RFQ samples sometimes showed a complete disappearance of the R1HS form just 50 ms after mixing, leaving just a small-intensity axial HS ferric heme EPR signal (not shown). We suggest that the reaction with H_2O_2 starts when the distal His55 is in the closed conformation. It is known that if a heme protein lacks a histidine in the distal side of the heme, the reaction can still be initiated, but Compound 0 (a transient complex of H_2O_2 and the ferric heme) is formed as the first intermediate.[21,34] Since no Compound 0 has been observed in DHP upon reaction with H_2O_2, it appears feasible that peroxide reacts with the heme iron when His55 is in the closed conformation. It is also known that the open, 5cHS, form of DHP is inactive and does not convert to compound ES.[16]

Once the oxoferryl heme state starts to be reduced in the course of the reaction, a new rhombic ferric species, R2HS, is formed with a slightly stronger rhombic distortion of the heme than in R1HS (Figure S7). This is likely to be an open His55 conformation of DHP, similar to R1HS but modified due to a peroxide-induced change in the heme geometry.

4.2. Compound I, Compound ES, and the Substrate Oxidation Site. Compound I is a term commonly used to describe the two-electron-oxidized form of a heme protein, in which one oxidizing equivalent originates from the ferric iron, resulting in the oxoferryl heme state, and the other comes from the π-system of the porphyrin, yielding a π-cation radical.

Compound I has not been reported in DHP. Instead, the oxidation state of DHP formed shortly after mixing with H_2O_2 has been interpreted as Compound ES[17] by analogy with C*c*P,[18] in which the heme is oxidized to the oxoferryl state and a free radical is formed on an amino acid. H_2O_2 reacting with respiratory heme proteins, such as Mbs and Hbs, also produces an oxoferryl heme state and a protein-bound radical. However, an essential difference with Compound ES in C*c*P is in the amount of the free radical produced. The apparent yield of the protein-bound free radical in the globins is never greater than a few percent.[22] We show now that in DHP the free radical concentration is nearly quantitative with respect to the enzyme concentration (a ~93% yield at 150 ms, pH 7, Figure 5). This fact makes the "oxoferryl + radical" oxidation state of DHP more like classical Compound ES in C*c*P rather than the "oxoferryl + radical" state in the globins.

We have assigned the Compound ES radical (the "principal radical") to either Tyr28 or Tyr34 on the basis of its EPR spectrum simulation (section 3.2.3). These two residues are both solvent-exposed and provide possible sites for electron transfer from the halogenated substrate. Of the two radical sites, Tyr34 is closer to the heme, and it makes a direct van der Waals contact with the heme porphyrin (Figure 8). This is one reason to suggest that the observed radical is on Tyr34. However, the other, more important reason is the fact that Tyr34 in DHP A is a conserved tyrosine residue in a number of globins, and structural homologues of this residue — Tyr103 in horse Mb, sperm whale Mb, and human Mb and Tyr42 in the α-subunit of human Hb — all are reportedly the sites of free radical formation when these globins react with H_2O_2.[22,35−38]

4.3. Effects of pH on the Reactivity of the Oxoferryl Heme. The oxoferryl heme must be in a dynamic equilibrium with its protonated state, which can be represented as the resonance hybrid boxed in Scheme 3.

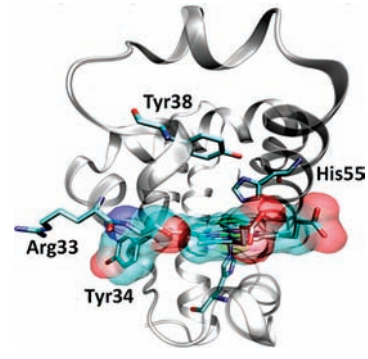

Figure 8. Selected residues in the heme environment of DHP. Tyr34, the site suggested to host the principal radical, is in van der Waals interaction with the heme porphyrin. Arg33 is in close proximity and might play a role in substrate binding. The pH 5 radical is proposed to be located on Tyr38, which can make a strong hydrogen bond with the distal His55. The PDB structure file 2QFK[10] was used to generate the figure.

(33) Nicoletti, F. P.; Thompson, M. K.; Howes, B. D.; Franzen, S.; Smulevich, G. *Biochemistry* **2010**, *49*, 1903–1912.
(34) Brittain, T.; Baker, A. R.; Butler, C. S.; Little, R. H.; Lowe, D. J.; Greenwood, C.; Watmough, N. J. *Biochem. J.* **1997**, *326*, 109–115.

Scheme 3

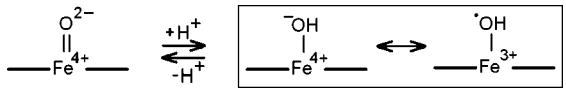

A direct correlation of Hb and Mb ferryl reactivity with their ferryl protonation status ($pK_a = 4.7$) has been demonstrated.[39] A value close to the pK_a for this equilibrium might be expected in DHP. Indeed, the state of the oxoferryl heme in DHP at pH 7 has been assessed by cryoreduction of DHP Compound ES with γ-radiation and was concluded to be a deprotonated $Fe^{4+}{=}O^{2-}$ state.[40]

The high oxoferryl reactivity in the protonated state can be understood from its electronic equivalence to a ferric heme iron coordinated by a hydroxyl radical (Scheme 3), the strongest oxidation agent known. The deprotonated oxoferryl heme, on the other hand, can be stable for hours.[41]

4.4. Hypothesis: Two Alternative Routes of the Reduction of the Protonated Oxoferryl Heme of Compound ES. The oxoferryl heme state, which is part of Compound ES, is chemically reactive and can be converted to the resting ferric state if it is protonated. It is electronically equivalent to a ferric heme iron coordinated by a hydroxyl radical (Scheme 3), which is a highly reactive oxidant. Therefore, we suggest that what happens after the oxoferryl is protonated depends on whether His55 is in the closed or open conformation.

If His55 is in the open conformation (higher population at the lower pH values, Figure 2), the protonated oxoferryl would abstract a hydrogen atom from the nearest target to be oxidized, the porphyrin (possibly in two steps, $-e^-$ and $-H^+$, as shown in the animation available for the open form in the Supporting Information). This would leave the porphyrin in a transient neutral free radical state, ready to recombine with the nearby neutral Tyr34 radical (principal radical), thus yielding a covalent cross-link between the tyrosine and the heme. Indeed, our HPLC data show the formation of a cross-link between the heme and the globin (Figures S8 and S9). Tyr34 is very close to the heme, and it is likely that it could form a cross-link. A homologous residue, Tyr103, in horse Mb treated with H_2O_2 was reported to form a cross-link with the heme,[42] although this assignment has been challenged.[43] Furthermore, an autocatalytic formation of a similar cross-link under H_2O_2 treatment has been demonstrated in ascorbate peroxidase in which a tyrosine has been engineered close to the heme edge.[44] The yield of the cross-link in DHP is higher at lower pH values (Figure 7), which is in agreement with a higher concentration of the protonated ferryl form of the heme and a higher concentration of the open His55 conformation. Therefore, we put forward a hypothesis that Compound RH is a ferric-type heme with the porphyrin covalently cross-linked to Tyr34. An important question is whether the formation of such a cross-link might be reversible, since it is known that Compound RH can be reduced by external reductants to the ferrous form of DHP.[17] The possibility that such a link in DHP can be reduced is supported by the fact that similar heme-to-protein cross-links in horse heart Mb[45] are partially reversible when sodium dithionite is used as a reductant (our unpublished data).

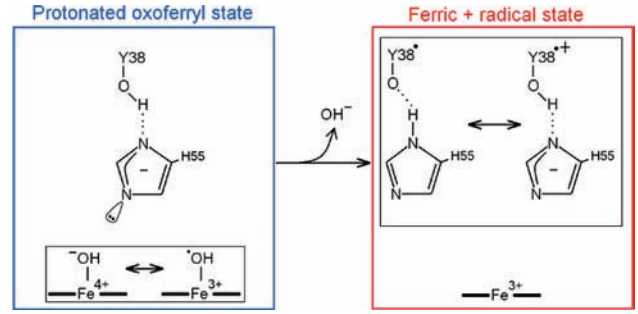

Figure 9. Conversion of the protonated oxoferryl heme to a "ferric heme + protein radical" state when the distal His55 is in the closed conformation. The Tyr38• radical is formed (the pH 5 radical), which might be in an equilibrium with its protonated form, the cation radical.

If, however, His55 is in the closed conformation (see the animation in the Supporting Information), which in terms of population is a much smaller fraction, the protonated ferryl would certainly attack the distal His55, likely by subtracting an electron from the lone pair of the imidazole's nitrogen (Figure 9). As a result, a hydroxyl anion will be liberated, the heme will be left in the ferric state, and a neutral radical will be formed on His55. What will happen next? We have assigned the EPR signal of the pH 5 radical to the neutral radical on Tyr38 (see section 3.2.3) on the basis of the EPR signal simulation and the DHP structure. We also concluded that the pH 5 radical must be strongly hydrogen bonded. Tyr38 is indeed very close to His55 when it is in the closed conformation (Figure 8) and can make a strong hydrogen bond with the nitrogen of the imidazole group.[10] Thus, it is reasonable to expect that the Tyr38 radical is formed instantly upon His55 oxidation by the protonated oxoferryl (Figure 9). A neutral Tyr38 radical might be in resonance with its cation radical when the proton is shared between the histidine and the tyrosyl radical, but the population of the latter state must be much smaller than the population of the neutral radical, which we observe as the pH 5 radical.

Thus, it appears that the dual functionality of DHP might be linked to changes in the enzyme's environment, particularly to the changes in the environment's oxidizing or reducing capacity. At decreased O_2 concentrations, the environment becomes more reducing and the ferrous heme fraction is increased. This shifts the DHP function toward oxygen binding. As oxygen becomes more abundant in the environment, spontaneous heme oxidation increases the ferric state DHP fraction, which can be seen as a shift toward the peroxidase function. This is useful in an oxidative environment, as such reactive oxygen species as H_2O_2 will be eliminated, and the trihalophenols will be converted to

(35) Fenwick, C. W.; English, A. M. *J. Am. Chem. Soc.* **1996**, *118*, 12236–12237.
(36) Harris, M. N.; Burchiel, S. W.; Winyard, P. G.; Engen, J. R.; Mobarak, C. D.; Timmins, G. S. *Chem. Res. Toxicol.* **2002**, *15*, 1589–1594.
(37) Gunther, M. R.; Sturgeon, B. E.; Mason, R. P. *Free Radic. Biol. Med.* **2000**, *28*, 709–719.
(38) Reeder, B. J.; Grey, M.; Silaghi-Dumitrescu, R. L.; Svistunenko, D. A.; Bulow, L.; Cooper, C. E.; Wilson, M. T. *J. Biol. Chem.* **2008**, *283*, 30780–30787.
(39) Silaghi-Dumitrescu, R.; Reeder, B. J.; Nicholls, P.; Cooper, C. E.; Wilson, M. T. *Biochem. J.* **2007**, *403*, 391–395.
(40) Davydov, R.; Osborne, R. L.; Kim, S. H.; Dawson, J. H.; Hoffman, B. M. *Biochemistry* **2008**, *47*, 5147–5155.
(41) Reeder, B. J.; Wilson, M. T. *Free Radic. Biol. Med.* **2001**, *30*, 1311–1318.
(42) Catalano, C. E.; Choe, Y. S.; Ortiz de Montellano, P. R. *J. Biol. Chem.* **1989**, *264*, 10534–10541.
(43) Reeder, B. J.; Cutruzzolà, F.; Bigotti, M. G.; Watmough, N. J.; Wilson, M. T. *IUBMB Life* **2007**, *59*, 477–489.
(44) Pipirou, Z.; Bottrill, A. R.; Svistunenko, D. A.; Efimov, I.; Basran, J.; Mistry, S. C.; Cooper, C. E.; Raven, E. L. *Biochemistry* **2007**, *46*, 13269–13278.
(45) Reeder, B. J.; Svistunenko, D. A.; Sharpe, M. A.; Wilson, M. T. *Biochemistry* **2002**, *41*, 367–375.

dihaloquinones on the way. However, if there are no trihalophenols in the environment, the two potentially damaging oxidative equivalents formed on DHP in the reaction with H_2O_2 recombine to form a safe heme-to-protein cross-link state, which is seen optically as Compound RH. According to this hypothesis, compound RH formation avoids a biradical state of DHP that would be highly reactive and potentially damaging. The yield of such a state is kept persistently low due to a low fraction of the His55 in the closed conformation at the low pH and to a low oxoferryl reactivity at the high pH values. Therefore, Compound RH is the state of DHP in an oxidative medium in the absence of substrates to oxidize. Once the environment becomes reducing again, the covalent link is reduced and Compound RH is transformed into oxyferrous heme DHP (Compound III).

Interestingly, whereas Compound RH has the heme in the ferric state, it cannot be further oxidized by H_2O_2.[17] This might be explained by suggesting that His55 is arrested in the open conformation in Compound RH, which makes it hardly possible for a H_2O_2 molecule to react with the heme.

Thus, DHP appears to be an oxygen-binding hemoglobin that becomes a peroxidase when oxygen concentration is increased. Alternatively, we could say that DHP is a peroxidase that switches to oxygen binding when the concentration of oxygen is decreased.

4.5. Analysis of the Optimized Rate Constants. The kinetic model used to fit experimental time dependences of the total free radical and total ferric heme states, at three different pH values, holds the following assumptions made on the basis of the experimental results obtained in this work:

(a) Formation of Compound ES takes place only when His55 is in the closed conformation.
(b) Open/closed His55 equilibrium is governed by a single protonation event.
(c) Compound ES decays only if the ferryl heme iron is protonated (although the *principal radical* associated with Compound ES can recombine with another radical in the system, independently of the heme oxidation state, thus turning Compound ES into a nonradical ferryl heme species).
(d) The ratio of the rates of the two alternative routes of the Compound ES decay directly depends on the open/closed His55 conformation: Compound RH is formed in the open conformation, but a second, *pH 5 radical* is formed in the closed conformation. Thus, the partial weight of these two routes of reaction (k_2/k_3) should have the same pH profile as the rate constant k_1 that reflects the pH dependence of Compound ES formation via reaction 1; that is, k_2/k_3k_1 is a constant at pH 5, 6, and 7.

When the kinetic model is optimized with the constraints imposed by the above assumptions, the calculated time dependences are found in satisfactory proximity to the experimental data points (Figures 4 and 5). The conclusions that follow from the analysis of the optimized rate constants further support the feasibility of the kinetic model and the molecular mechanism of the reaction.

Figure 10 shows the pH dependences of the optimized rate constants (Table 2). The k_1 dependence on pH is in agreement with the EPR data on the pH dependence of the R1HS and NAHS equilibrium (Figure 2). Also, the values of k_1 obtained from the model are in agreement with the Compound ES formation rate constants determined for pH 5 and pH 7 by optical spectroscopy (2.78×10^4 and 3.56×10^4 M^{-1} s^{-1} at pH 5 and 7, respectively[17]). An estimate of the pK_a value from the *Step* parameter defined from the three k_1 values optimized for pH 5, pH 6, and pH 7 (SI.Results.3) give a value of 6.9. Interestingly, a similar equilibrium between the 5cHS (open) and 6cHS (closed) heme states in Mb, which is characterized by orders of magnitude lower peroxidase activity, is observed at a significantly lower pK_a of 4.5.[46]

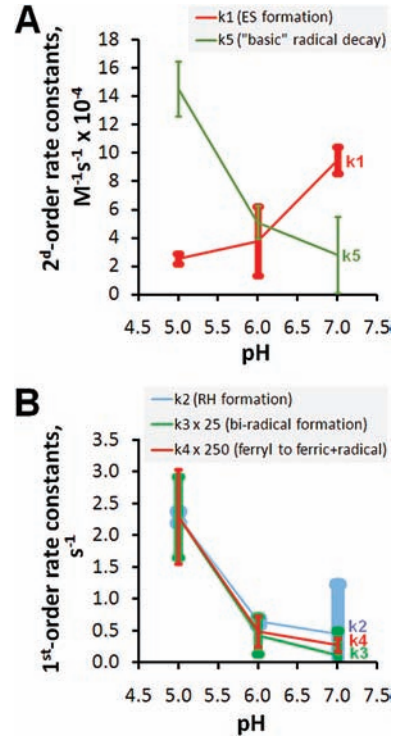

Figure 10. Optimized values of the second-order (A) and first-order (B) rate constants used in the kinetic model (see section 3.2.5) plotted as functions of pH. For comparative viewing, k_3 and k_4 dependences (B) are multiplied by the factors of 25 and 250, respectively, to bring the pH 5 data point to a similar position on the graph. Rate constants k_6-k_{10} are set in the model to be proportional to k_5, and therefore they have pH dependences identical in shape to that of k_5 and are not shown. The error bars indicate how much the rate constants should be changed (individually, while keeping the other constants at the optimized values) in order to produce a 1 μM increase in the global "target" optimization parameter *T*.

We interpret Compound RH of DHP as a ferric heme state with the heme covalently bound to the globin. In agreement with this, the rate constants k_2 of Compound RH formation at the three pH values (Figure 10B) correlate with the yield of the heme-to-protein cross-links (Figure 7). The values of k_2 obtained from the model are approximately 30 times greater than the rates of Compound RH formation determined optically (0.0701 s^{-1} at pH 5 and 0.0167 s^{-1} at pH 7),[17] although both sets of data have similar pH trends. If these differences are confirmed in future experiments under common reaction conditions, it might indicate that what we see kinetically as the principal radical disappearance linked to the ferric heme state formation is not formation of Compound RH but rather formation of its precursor, which then transforms to Compound RH with an approximately 30-fold slower rate.

The radical decay rate constants, as determined from the model (Figure 10A), decrease with increasing pH (with a formal pK_a = 5.2 estimated from the *Step* parameter for the three "basic" radical decay rate constants k_5; see SI.Results.3 for

(46) Yang, F.; Phillips, G. N., Jr. *J. Mol. Biol.* **1996**, *256*, 762–774.

details). This is in agreement with a faster loss of the hyperfine structure in the free radical EPR spectrum at the lower pH values (see section 3.2.1). Even quantitative comparison shows a good correlation: while $k_5^{pH6}/k_5^{pH7} = 1.8$, the rate of loss of the hyperfine structure in the EPR spectra (estimated as inverse time of the line shape preservation; see section 3.2.1) is 2 times greater at pH 6 than at pH 7; also, while $k_5^{pH5}/k_5^{pH6} = 2.8$, the rate of loss of the hyperfine structure at pH 5 is 6 times greater than at pH 6. We think that such a good quantitative agreement is remarkable, particularly since no information about the free radical spectra line shape is present the kinetic model.

Finally, the overall rate of the oxoferryl heme decay ($k_2 + k_3 + k_4$) has a pH profile consistent with $pK_a = 4.4$ (see Excel file in Supporting Information), a value which is very close to the $pK_a = 4.7$ for the globins' oxoferryl heme protonation.[39] Reaction 4, however, contributes very little to the overall sum (0.2−0.4%; note that the k_4 dependence is multiplied by a factor of 250 in Figure 10B).

Overall, the kinetic model that satisfactorily describes the experimental data is dependent on three pK_a values roughly estimated from the triads of the rate constants optimized at pH 5, pH 6, and pH 7. The first one, $pK_a = 6.9$, is related to the His55 protonation and thus governs its open/closed conformations. The second, $pK_a = 4.4$, defines if the oxoferryl heme is protonated and therefore redox active. The third one, $pK_a = 5.2$, governs the radical decay and is suggested to reflect the radical-transfer dependence on the pH.

5. Conclusions

1. Two HS ferric heme forms are found in the resting enzyme and assigned to the 6cHS (aquo) heme with the distal His55 in the closed conformation and the 5cHS heme with His55 in the open conformation.

2. Two free radicals are identified in DHP activated by H_2O_2. The one associated with Compound ES has been assigned to the on-surface residue, Tyr34. The other radical, better detectable at lower pH values, has been assigned to Tyr38, which is well situated to make a strong hydrogen bond with the distal histidine, His55.

3. Covalent heme-to-protein cross-links are found in DHP treated with H_2O_2.

4. A pH-dependent mechanism of DHP activation by H_2O_2 is proposed and tested by kinetic modeling. A good correspondence between the model and the experimental data, at a range of pH values, allows the following interpretation of the results obtained. The formation of Compound ES is pH dependent, reflecting the pH dependence of the equilibrium of the distal His55 in the open and closed conformations. Once formed, Compound ES may enter one of the two alternative paths of further transformation. This depends again on whether His55 is in the closed or in the open conformation. In the less populated closed conformation, the Tyr38 radical is formed, but in the major open conformation, if no trihalophenol substrates are available, the protonated oxoferryl produces a transient porphyrin radical, which recombines with Tyr34$^{\bullet}$ and makes a heme-to-protein cross-link. This cross-link might be the Compound RH characterized previously by optical spectroscopy, or it might be its precursor. Formation of Compound RH is therefore interpreted as the enzyme's means to terminate the two oxidizing equivalents in a safe way, producing a cross-linked heme, which can be further reduced in a controlled way. Thus, the ability of H_2O_2-activated DHP to be transformed into a safe state of Compound RH might be important in avoiding unwanted radical propagation in the absence of trihalophenol substrates.

Acknowledgment. D.A.S. acknowledges the BBSRC grant BB/E02355X/1 "Advanced sample making tools for electron paramagnetic resonance spectroscopy". S.F. and M.K.T. acknowledge support by the Army Research Office grant 52278-LS.

Supporting Information Available: Details of new freeze-quenching apparatus, EPR spectra correction for variable length of EPR samples, spectra shifting in accordance with the microwave frequency, and assignment of radicals to specific tyrosine residues; supporting figures and tables; kinetic model Excel file; Quicktime animations of electron and proton transfer in open and closed His55 conformations. This material is available free of charge via the Internet at http://pubs.acs.org.

JA106620Q